

## EURECA: European-Japanese Microcalorimeter Array

**P. de Korte · J. Anquita · F. Bakker · X. Barcons · P. Bastia · J. Beyer · D. Boersma · F. Briones · M. Bruijn · J. Bussons · A. Camòn · F. Carrera · M. Ceballos · L. Colasanti · D. Drung · L. Fabrega · L. Ferrari · F. Gatti · R. Gonzalez-Arrabal · L. Gottardi · W. Hajdas · P. Helistö · J.W. den Herder · H. Hoevers · Y. Ishisaki · M. Kiviranta · J. van der Kuur · C. Macculi · A. Mchedlishvili · K. Mitsuda · B. Monna · R. Mossel · T. Ohashi · S. Pantali · M. Parra · L. Piro · R. Rohlfs · J. Sésé · Y. Takei · G. Torrioli · H. van Weers · N. Yamasaki**

Received: 23 July 2007 / Accepted: 5 October 2007 / Published online: 28 February 2008  
© Springer Science+Business Media, LLC 2008

---

P. de Korte (✉) · F. Bakker · D. Boersma · M. Bruijn · L. Gottardi · J.W. den Herder · H. Hoevers · J. van der Kuur · R. Mossel · Y. Takei · H. van Weers  
SRON Netherlands Institute for Space Research, Sorbonnelaan 2, 3584 CA Utrecht, Netherlands  
e-mail: P.de.Korte@sron.nl

J. Anquita · F. Briones · R. Gonzalez-Arrabal  
IMM-CSIC, Madrid, Spain

X. Barcons · J. Bussons · F. Carrera · M. Ceballos  
IFCA, Santander, Spain

J. Bussons  
University of Murcia, Murcia, Spain

A. Camòn · M. Parra  
IMCA, Zaragoza, Spain

J. Sésé  
INA, Zaragoza, Spain

L. Fabrega  
IMM-CSIC, Barcelona, Spain

W. Hajdas · A. Mchedlishvili  
PSI, Villigen, Switzerland

L. Ferrari · F. Gatti  
INFN/University of Genoa, Genoa, Italy

P. Bastia  
Thales Alenia Spazio, Milano, Italy

L. Colasanti · C. Macculi · L. Piro  
IASF/INAF, Rome, Italy

**Abstract** The EURECA project aims to demonstrate technological readiness of a micro-calorimeter array for application in future X-ray astronomy missions, like Constellation-X, EDGE, and XEUS. The prototype instrument consists of a  $5 \times 5$  pixel array of TES-based micro-calorimeters read out by two SQUID-amplifier channels using frequency-domain-multiplexing (FDM) with digital base-band feedback. The detector array is cooled by a cryogen-free cryostat consisting of a pulse tube cooler and a two stage ADR. Initial tests of the system at the PTB beam line of the BESSY synchrotron showed stable performance and an X-ray energy resolution of 1.5 eV at 250 eV for read-out of one TES-pixel only. Next step is deployment of FDM to read-out the full array. Full performance demonstration is expected end 2008.

**Keywords** X-ray microcalorimeters · Transition edge sensors · Frequency-domain-multiplexing

**PACS** 07.20.Fw · 85.25.Am · 85.25.Dq · 85.25.Oj · 95.55.-n.

## 1 Introduction

The core of the EURECA [1] proto-type instrument consists of a  $5 \times 5$  pixel micro-calorimeter array based on Ti/Au transition-edge-sensors (TES) [2] optimized for the 0.1–3 keV energy range. The EURECA project aims to demonstrate flight readiness for future X-ray astronomy missions, like EDGE and XEUS in Europe, NEXT and DIOS in Japan, and Constellation-X in the United States. The required energy resolution is 1 eV @ 1 keV, and the signal fall time  $< 100 \mu\text{s}$ . The instrument is cooled by a cryogen-free system based on a 4 K pulse tube cooler and a double stage ADR

---

G. Torrioli  
IFN-CNR Rome, Rome, Italy

P. Helistö · M. Kiviranta  
VTT-Sensors, Espoo, Finland

J. Beyer · D. Drung  
PTB, Berlin, Germany

Y. Ishisaki · T. Ohashi  
Tokyo Metropolitan University, Tokyo, Japan

K. Mitsuda · R. Rohlfs · N. Yamasaki  
ISAS/JAXA, Tokyo, Japan

B. Monna  
Systematic Design B.V., Delft, Netherlands

S. Pantali  
ISDC, Versoix, Switzerland

with 800 and 60 mK. Such a cooler is representative for space-type coolers, so that potential performance degradation due to EMI and vibrations from the pulse tube and magnetic fields from the ADR can be assessed.

The instrument will be read-out by two SQUID-based amplifier chains making use of frequency-domain-multiplexing [3, 4]. The instrument has been designed such that flexibility exists to test different SQUIDS and low-noise amplifier chains, as well as various ways to implement the required flux-locked-loop feedback. This modularity allows to test and use components provided for by international partners in the EURECA project.

## 2 System Design, EMI and Microphony

The high energy resolution of a TES-based micro-calorimeter requires extreme care in the protection of the sensor and its read-out electronics against EMI and microphony from other parts of the instrument and its environment. Levels of fW absorbed at the TES degrade the performance. The system design (Fig. 1) is characterized by: single point grounding inside the front-end-electronics (FEE); separation of analogue and digital electronics; integration of FEE, cold head (TES-array, LC-filters, and SQUIDS), and cryogenic harness inside one Faraday cage; filtering of all cable lines at 4 K (entrance SC-shield) and at entrance to FEE-box; 2-stage shielding of cold head; and optical links to PC and Internet. In addition the valve-head

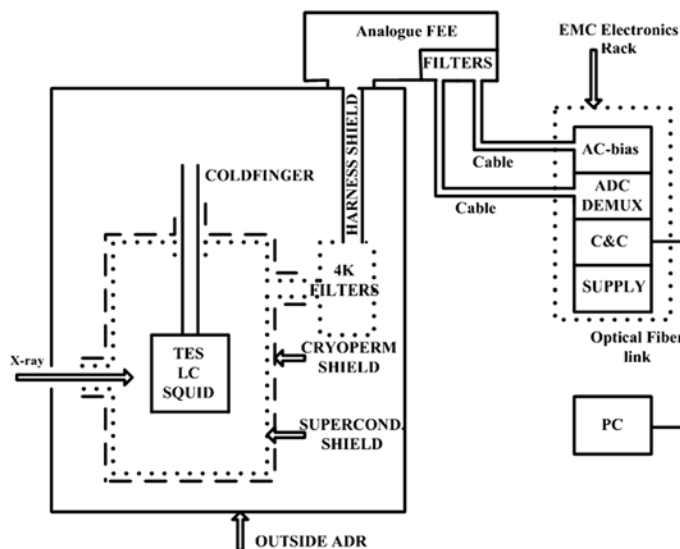


**Fig. 1** System design. The cold head of the instrument (TES-array, LC-filters, and SQUIDS) is shielded by a cryoperm and superconducting (SC) shield at 4 K. The superconducting shield extends into the 4 K filter box. Connections between the analogue (FEE) and digital electronics is through shielded cables and a filter unit at the entrance of the FEE-box. The connections to the outside world (e.g. PCs) is by optical fibres

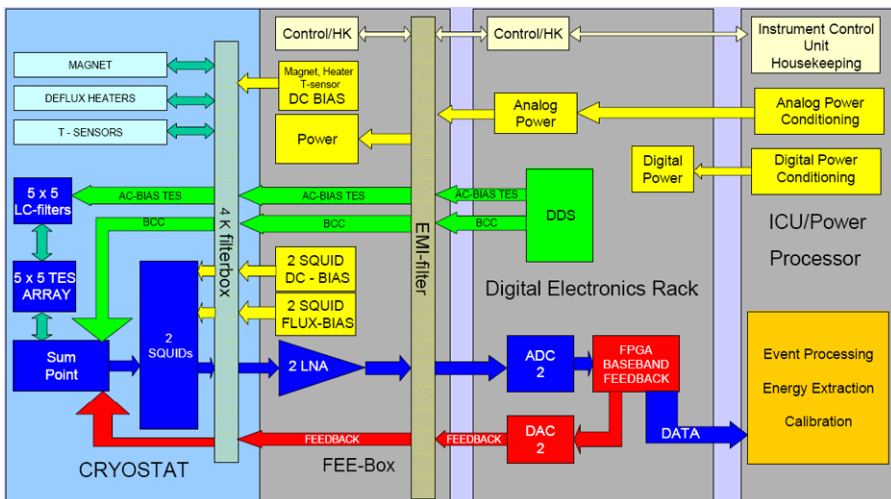


**Fig. 2** (Color online) Electronics Block diagram for EURECA. Base-band feedback is incorporated to extend the dynamic range of the SQUID-amplifiers

of the pulse tube cooler has been removed from the pulse tube/cryostat, thereby enabling galvanic separation of that unit from the cryostat. To minimize vibration input from the compressor onto the cooler the pressure hoses have been fixated rigidly before connection to the pulse tube. Last spring, stable performance of this system has been demonstrated at the PTB beam line of the BESSY synchrotron showing 1.5 eV FWHM energy resolution at 250 eV, and < 2 eV up to 1.8 keV [5]. In this test the FEE electronics consisted of commercial SQUID electronics for the read-out of one DC-biased pixel of the array.

Next step is the integration of the FDM electronics into the system with as baseline the use of base-band feedback (see Fig. 2).

### 3 Signal Summing, TES-Bias Topology, and Cold Head

The baseline topology for FDM is current summing (Fig. 3), but also flux-summing by making use of a multi-input Seiko SQUID [6] will be assessed. For EURECA a frequency-comb will be used to bias the TESs for one channel, since this allows for adjustment of the bias frequencies to the central frequency of each LC-filter. Very clean (<120 dBc @ 1 kHz from carrier) AC-bias signals are produced by Direct-Digital-Synthesis (DDS) chips for now and by special developed ASICs in the future. For voltage bias the equivalent series resistance  $R_{ESR} = \omega L / Q$  of the LC-filters has to be significant smaller than the TES bias resistance  $R_{TES}$ . For  $R_{TES} = 40 \text{ m}\Omega$  and  $L = 600 \text{ nH}$ , compatible with a signal of 100  $\mu\text{s}$  fall-time it is required that  $Q \gg 100 f$  (MHz). LC-filters made of Nb and  $\text{Al}_2\text{O}_3$  dielectric have already shown  $Q \approx 4000$  measured at 2.6 MHz [2]. The input coil of the SQUID acts as a common impedance  $\omega L_C$  and causes current cross-talk [7] at the level  $(L_C/2L) \times (f/\Delta f)$ . At a bias frequency  $f = 10 \text{ MHz}$ ,  $\Delta f = 0.2 \text{ MHz}$ , and  $L = 600 \text{ nH}$  we require that

**Fig. 3** The TESs current outputs are summed at the input coil of the SQUID amplifier. Each TES is AC-biased at the central frequency of its LC-filter, required to stop addition of wide-band Johnson noise. The bias frequencies are supplied as a frequency-comb, and coupled by bias-capacitors. Bias-current cancellation (BCC) and feedback are fed to the sum point

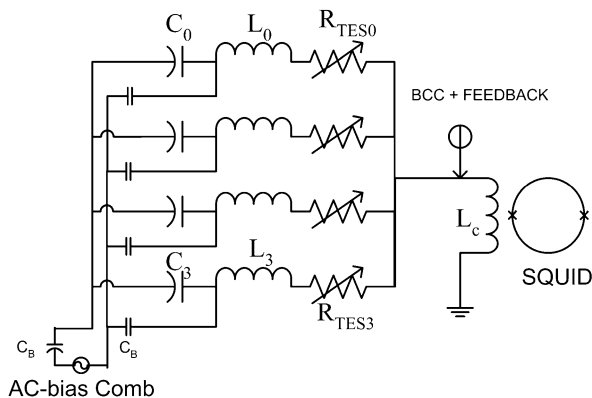
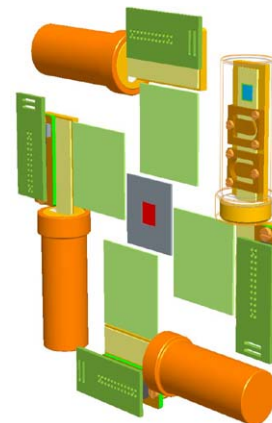


**Fig. 4** (Color online) Design of cold head. The central  $5 \times 5$  pixel array is surrounded by 4 LC-filter chips (green), and 4 SQUID units with interconnection boards



$L_C < 0.24$  nH to meet the goal of  $10^{-4}$  power cross-talk to a neighboring frequency pixel.

The baseline PTB 16-SQUID array [8] has an input inductance  $< 3$  nH, so flux-locked-loop (FLL) feedback with a gain of at least  $12\times$  is required to meet this criterion. The cold head of EURECA comprises a  $5 \times 5$  pixel array, 4 LC-filter chips for 8 pixels each, and 4 SQUIDs. Of these SQUIDs two can be connected to the harness and room temperature electronics. At this stage a planar geometry (Fig. 4) has been chosen.

#### 4 FDM Frequency Range and Channel Separation

The channel separation is driven by the information bandwidth in each pixel (about 10 kHz for EURECA), the cross-talk level allowed for (about  $10^{-3}$ ), and the way of biasing. Crosstalk levels  $< 10^{-3}$  can be obtained for  $\Delta f > 75$  kHz, when row biasing is used. This type of biasing requires that the filters in one row are tuned to the same frequency. In case of biasing with a frequency-comb, the baseline for EURECA, the filters themselves have to separate the frequencies over the pixels,

which due to the finite filter steepness leads to multi-frequency biasing of each pixel. In that case  $\Delta f > 200$  kHz for a crosstalk levels  $< 10^{-3}$ .

The frequency range that can be used for FDM is limited at the low frequency end by the capacitor size of the LC-filter, and at the high frequency end by the  $Q$  of the LC-filter and the back-action noise of the SQUID. For  $L = 600$  nH coils, consistent with our present pixels ( $R_N = 0.2$   $\Omega$ ,  $\beta = 1$ , and  $\tau = 100$   $\mu\text{s}$ ) we require  $C = 42$  nF @  $f = 1$  MHz. For our Nb/Al<sub>2</sub>O<sub>3</sub>/Nb capacitors (3.4 nF/mm<sup>2</sup>) this would require a  $3.5 \times 3.5$  mm<sup>2</sup> capacitor. So about 1 MHz seems to be a lower limit. At higher frequencies the  $Q$ -factor is a potential limit. For 10 MHz we require  $Q \gg 1000$ . So far we have realized filters with  $Q \approx 4000$ . Another high frequency limitation is back-action noise from the SQUID. Theoretically input noise and back-action noise are about equal for  $\omega = R_{\text{TES}} \cdot L_{\text{SQ}} / NM^2 = R_{\text{TES}} / n^2 N L_{\text{SQ}}$  with  $L_{\text{SQ}}$  the SQUID inductance,  $M$  the mutual input inductance,  $N$  the number of SQUIDs in the array, and  $n$  the number of turns on the input coil. For the 16-SQUID PTB array [8], presently the baseline for EURECA, that frequency is about 10 MHz for  $R_{\text{TES}} = 40$  m $\Omega$ . For now we assume a maximum operating frequency of 10 MHz.

So about 9 MHz frequency range is available for FDM. Using 200 kHz channel separation 45 pixel can be multiplexed in one SQUID-channel. In case of row bias, the use of 100 kHz separation is feasible, which enables multiplexing of as much as 90 pixels in one channel.

## 5 Dynamic Range, Linearity, and Base-Band Feedback

X-ray micro-calorimeters require a large dynamic range for their electronics. For EURECA ( $E_{\text{MAX}} = 3$  keV,  $\Delta E = 1$  eV) an electronics dynamic range of  $\pm 3 \times 10^6 \sqrt{\text{Hz}}$  is needed for one pixel. The dynamic range required for the maximum signal in one chain of multiplexed pixels is about the same, since the likelihood of coincident large events is extremely small for X-ray astronomy. This means that FDM applied for X-ray astronomy doesn't suffer much from the multiplex disadvantage present in TDM. Good SQUIDs have a typical flux noise of  $0.1\text{--}0.2 \mu\phi_0/\sqrt{\text{Hz}}$  and a maximum range of  $\pm 0.2\phi_0$ , giving a full dynamic range of about  $\pm(1\text{--}2) \times 10^6 \sqrt{\text{Hz}}$ . So feedback is required to increase the SQUID dynamic range as well as to linearize its response.

Nonlinearity does not only result in a nonlinear response, but also in the creation of higher order signals that might create crosstalk with channels biased at other frequencies. For typical SQUID nonlinearities a FLL-gain of about  $50\times$  is required to keep the higher order mixing terms below  $10^{-4}$  of the linear term. Since the gain-bandwidth product of a FLL system is limited by cable delay and amplifier bandwidth high FLL-gains are not possible for FDM carrier frequencies in the MHz range. Since the carriers themselves do not contain relevant information it should be possible to create feedback for the information bandwidth of the signals (10 kHz) only. This so-called base-band feedback can be incorporated by de-modulation and re-modulation of the signal before feedback, so that the phase difference of the carriers can be compensated for (Fig. 5). Since most of the energy content of the pulse is at frequencies  $< 10$  kHz the  $50\times$  gain in the FLL requires a gain-bandwidth of 500 kHz at the baseband. The gain-bandwidth at base-band has been measured on a breadboard consisting of sum point, ADC, FPGA, and DAC with 4 carriers in the 1–10 MHz range. The

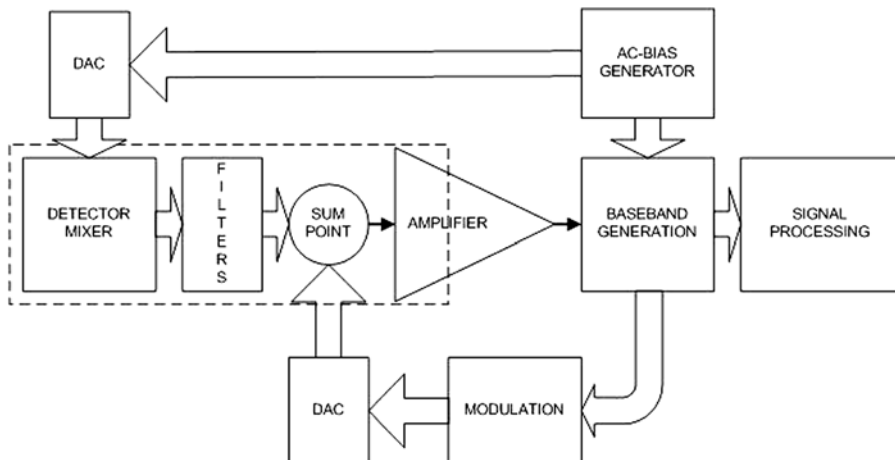


**Fig. 5** Conceptual design for FDM with base-band feedback. The de- and re-modulation is implemented digitally

measured 200 kHz is close to the 160 kHz expected on basis of the 770 ns delay in ADC, FPGA, and DAC of the present breadboard. Systems with about 250 ns delay and 500 kHz gain-bandwidth are quite well possible.

## 6 Conclusion

The 1st phase of the EURECA project has been finished successfully with a campaign at the BESSY synchrotron and good performance of base-band feedback on an electronic breadboard. In the coming year a start will be made with FDM read-out of the  $5 \times 5$  pixel array finished by a BESSY campaign that aims to read-out 8 pixels in one FDM SQUID channel with high energy resolution.

**Acknowledgement** This work was financially supported by the Dutch Organization for Scientific Research (NWO).

## References

1. P.A.J. de Korte et al., Proc. SPIE **6266**, 62661 (2006)
2. M.P. Bruijn et al., J. Low Temp. Phys. (2008). doi:[10.1007/s10909-007-9681-6](https://doi.org/10.1007/s10909-007-9681-6)
3. M. Kiviranta et al., in *AIP Conf. Proc. LTD-9 605*, ed. by F. Porter, D. McCammon, M. Galeazzi, C. Stahle (2001), pp. 295–300
4. T.M. Lanting et al., Appl. Phys. Lett. **86**, 112511 (2005)
5. L. Gottardi et al., J. Low Temp. Phys. (2008). doi:[10.1008/s10909-007-9629-x](https://doi.org/10.1008/s10909-007-9629-x)
6. N. Yamasaki et al., IEICE Trans. Electron. **E89-C**, 98 (2006)
7. J. van der Kuur et al., in *Proc. LTD-10*, ed. by F. Gatti. Nucl. Instrum. Methods **520**, 551 (2004)
8. J. Beyer et al., these proceedings